Chemistry Research Journal, 2017, 2(1):27-41

Available online www.chemrj.org

Research Article

ISSN: 2455-8990
CODEN(USA): CRJHA5

Dissecting the drug-receptor interaction with the Klopman-Peradejordi-Gómez (KPG) method. I. The interaction of 2,5-dimethoxyphenethylamines and their *N*-2-methoxybenzyl-substituted analogs with 5-HT_{1A} serotonin receptors

Juan S. Gómez-Jeria*, Camila Moreno-Rojas

Quantum Pharmacology Unit, Department of Chemistry, Faculty of Sciences, University of Chile. Las Palmeras 3425, Santiago 7800003, Chile

Abstract We studied the relationships between electronic structure and 5-HT_{1A} receptor binding affinity of a group of 2,5-dimethoxyphenethylamines and their N-2-methoxybenzyl-substituted analogs. The novelty of this study is that we analyzed four hypothesis about the mode of binding, leading to four different common skeletons. For all cases statistically significant equations were obtained, each one leading to a partial interaction pharmacophore. The integration of all the results into a unique pharmacophore that provides more detailed information about the mode of binding of these molecules to the 5-HT_{1A} receptor.

Keywords 5-HT_{1A}, serotonin, QSAR, common skeleton, DFT, electronic structure, Phenethylamines, N-2-methoxy-phenethylamines, Pharmacophore

Introduction

The Klopman-Peradejordi-Gómez (KPG) method relating electronic structure and biological activity is, as far as we know, the only member of the class of model-based methods. It starts from the statistical mechanical definition of the equilibrium constant [1]. Then, by applying physically reasonable hypotheses it produces a relationship between local atomic reactivity indices and the drug-site equilibrium constant. This model has been enlarged through the years. The first version was proposed by Peradejordi et al. including the treatment of the drug-site interaction energy [2]. Later the contribution of the molecular partition functions was analyzed [1]. After this, the drug-site interaction energy was again analyzed giving origin to a group of reactivity indices related to the Molecular Orbitals (MOs) [3]. The next step was the analysis of the molecular rotational partition function giving origin to the orientational parameters [4]. During year 2013 a new analysis of the drug-site interaction energy gave origin to local atomic indices such as local atomic hardness, local atomic softness, local atomic electrophilicity, etc. [5, 6]. These local atomic indices looked like the ones coming from conceptual density functional theory but they are conceptually different from them because their units are the same than the global indices. The last development was the guess, based on studies published during years 1965-1975, that this equation can be applied to any biological activity, provided that all molecules have the same action mechanism [7]. The results of the application of this method have been excellent when applied to several molecular systems and biological activities (see [8-22] and references therein). Considering that the method has been explained with detail in many papers and one freely available book, we refer the reader to the literature (all the papers and the book can be found at www.researchgate.net).

The practical application of the KPG method is difficult by the fact that no research group has ever published a paper with enough molecules to solve the KPG linear equation system of equations. To circumvent this problem, we made use of linear multiple regression analysis to find the main factors controlling the variation of receptor binding in a group of molecules. Statistics is used here as a slave and not as a master. Then, and from a philosophical point of view, this method is totally unrelated to those based on the equation: "*Any biological activity I want to study = a combination of all classical and quantum chemical parameters at my hand*" and using statistics to see if there is a statistically significant result.

Usually, the KPG method makes use of the concept of *common skeleton*. This skeleton is defined as a definite collection of atoms, common to all molecules selected for a study, which accounts for nearly all the receptor binding. The action of the substituents consists in modifying the electronic structure of the common skeleton and influencing the right alignment of the drug throughout the orientational parameters. Now, let us consider a molecular system depicted below.

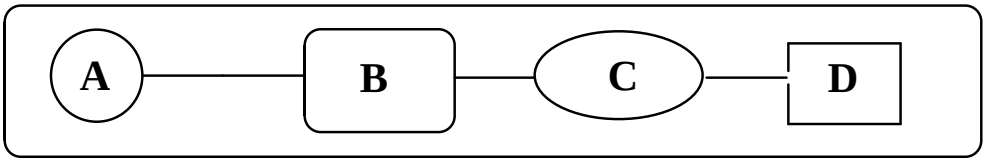

This system is arbitrarily divided in regions A, B, C and D that are common to all molecules studied. The common skeleton contains atoms belonging to all of them. The standard KPG procedure employs this skeleton. Now, let us consider that case in which all molecules have regions A, B and C in common (set X), but region D is present only in some of them (set Y). In these cases the KPG method can be applied to two sets of molecules: the one corresponding to set X and the one composed by set X plus set Y. In the first case we use atoms of regions A, B and C to compose the common skeleton and in the second we employ atoms of the four regions. The analysis of the statistically significant results should provide more information about some of the atoms participating in the drug-receptor interaction. To test this approach, we present here the results of a study relating the electronic structure of some 2,5-dimethoxyphenethylamines and their *N*-2-methoxybenzyl-substituted analogs with 5-HT_{1A} serotonin receptors considering several definitions of the common skeleton. These molecules and receptor were selected because we carried out several studies on serotonin receptors and related molecules [23-30]. Another reason is that the molecules have psychoactive effects and it is of interest to compile information about their mode on binding to their receptors. Considering what we said above about the method we shall discuss in this paper only the results.

Calculations

The molecules and receptor binding results were taken from a recent publication [31], and are presented in Fig. 1 and Table 1. The binding affinities were measured in membrane preparations of human embryonic kidney (HEK) 293 cells overexpressing the 5-HT_{1A} receptors (human genes).

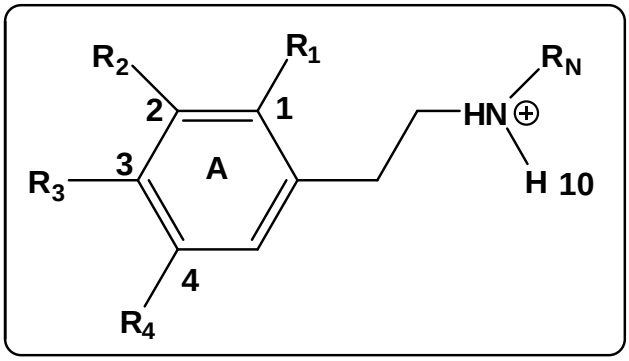

Figure 1: General formula of molecules used in this study

Table 1: 2,5-dimethoxyphenethylamines, their N-2-methoxybenzyl-substituted analogs and receptor binding.

Molecule	R_1	R_2	R_3	R_4	R_N	$\log(K_i)$ $5HT_{1A}$
1	OMe	H	Br	OMe	H	-0.62
2	OMe	H	Cl	OMe	H	-0.72
3	OMe	H	Me	OMe	H	-0.36
4	OMe	H	Et	OMe	H	-0.44
5	OMe	H	Br	OMe	2-methoxybenzyl	0.56
6	OMe	H	Cl	OMe	2-methoxybenzyl	0.70
7	OMe	H	Me	OMe	2-methoxybenzyl	0.85
8	OMe	H	Et	OMe	2-methoxybenzyl	0.54
9	OMe	H	H	OMe	H	-1.15
10	OMe	H	I	OMe	H	-0.74
11	OMe	H	NO_2	OMe	H	0.34
12	OMe	H	*n*-Pr	OMe	H	-0.96
13	OMe	H	H	OMe	2-methoxybenzyl	0.78
14	OMe	H	I	OMe	2-methoxybenzyl	0.26
15	OMe	H	NO_2	OMe	2-methoxybenzyl	0.62
16	OMe	H	*n*-Pr	OMe	2-methoxybenzyl	0.26
17	OMe	H	SEt	OMe	H	-0.43
18	OMe	H	S-*i*-Pr	OMe	H	-0.33
19	OMe	H	S-Pr	OMe	H	-0.28
20	H	OMe	OMe	OMe	H	0.66
21	OMe	H	SEt	OMe	2-methoxybenzyl	0.34
22	OMe	H	S-*i*-Pr	OMe	2-methoxybenzyl	0.40
23	OMe	H	S-*i*-Pr	OMe	2-methoxybenzyl	0.26
24	H	OMe	OMe	OMe	2-methoxybenzyl	1.32

The common skeleton

We considered four possibilities for the building of the common skeleton (see Fig. 1):

Case 1. We hypothesized that all 24 molecules interact with the $5HT_{1A}$ receptor only through the aromatic ring A, the alkylamino chain and the proton.

Case 2. We hypothesized that all 24 molecules interact with the $5HT_{1A}$ receptor only through the aromatic ring A, the alkylamino chain, the proton and the first atom of the substituents attached to positions 1-4.

Case 3. We hypothesized that all 12 *N*-2-methoxyphenyl-phenethylamines interact with the $5HT_{1A}$ receptor only through the aromatic ring A, the alkylamino chain, the proton, the first atom of the substituents attached to positions 1-4 and the methoxyphenyl moiety (including the first atom of the methoxyphenyl substituent).

Case 4. We hypothesized that all 12 phenylalkylamines interact with the $5HT_{1A}$ receptor only through the aromatic ring A, the alkylamino chain, the proton and the first atom of the substituents attached to positions 1-4 (see below for each common skeleton).

Calculations

The electronic structure of all molecules was calculated within the Density Functional Theory (DFT) at the mPW1PW91/DGDZVP level with full geometry optimization [32]. The protonated forms were used. The Gaussian suite of programs was used [33]. The information needed to calculate the numerical values for the LARIs was obtained from the Gaussian results with the D-Cent-QSAR software [34]. All the electron populations smaller than or equal to 0.01 e were considered as zero. Negative electron populations coming from Mulliken Population Analysis were corrected as usual [35]. Orientational parameters taken from published Tables or calculated as usual [36-38]. Since the resolution of the system of linear equations is not possible because we have not experimental

data, we employed Linear Multiple Regression Analysis (LMRA) techniques to find the best solution. For each case, a matrix containing the dependent variable ($\log(IC_{50})$ in this case) and the local atomic reactivity indices of all atoms of the common skeleton as independent variables was built. Regarding the local atomic reactivity indices depending on the MO (Fukui indices and superdelocalizabilities) we have employed only those associated with the frontier local molecular orbitals. The Statistica software was used for LMRA [39].

Results

Results for Case 1. The common skeleton for this case is shown below (Fig. 2).

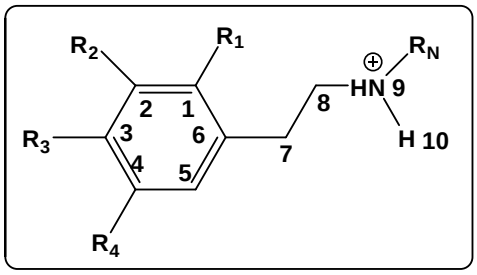

Figure 2: Common skeleton numbering for case 1

The best equation obtained was:

$$\log(IC_{50}) = 0.24 + 1.97 S_7^N(LUMO)^* - 18.82 S_8^E(HOMO)^* - 0.002 S_1^N \quad (1)$$

with n=21, R=0.98, R^2=0.96, adj-R^2=0.95, F(3,17)=121.93 (p<0.000001) and SD=0.13. No outliers were detected and no residuals fall outside the ±2σ limits. Here, S^N_7(LUMO)* is the nucleophilic superdelocalizability of the lowest vacant MO localized on atom 7, S^E_8(HOMO)* is the electrophilic superdelocalizability of the highest occupied MO localized on atom 8 and S_1^N is the total atomic nucleophilic superdelocalizability of atom 1. Tables 2 and 3 show the beta coefficients, the results of the t-test for significance of coefficients and the matrix of squared correlation coefficients for the variables of Eq. 1. There are no significant internal correlations between independent variables (Table 3). Figure 3 displays the plot of observed *vs.* calculated $\log(IC_{50})$.

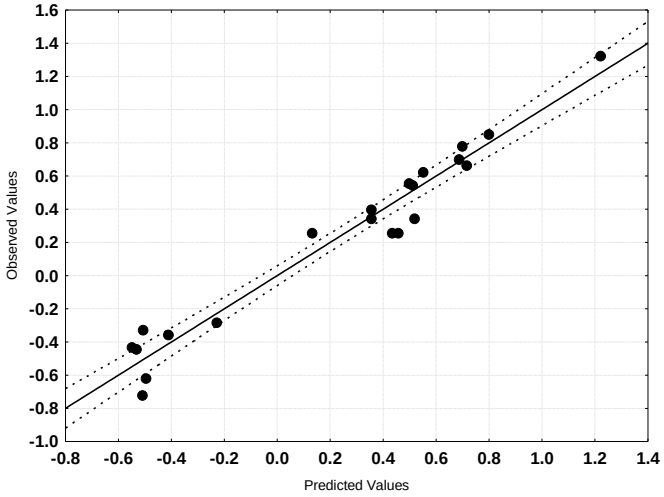

Figure 3: Plot of predicted vs. observed log(K_i) values (Eq. 1). Dashed lines denote the 95% confidence interval

Table 2: Beta coefficients and t-test for significance of coefficients in Eq. 1

Var.	Beta	t(17)	p-level
S^N_7(LUMO)*	0.85	16.19	<0.000001
S^E_8(HOMO)*	-0.34	-5.32	<0.00006
S_1^N	-0.21	-3.18	<0.006

Table 3: Matrix of squared correlation coefficients for the variables in Eq. 1

	S^N_7(LUMO)*	S^E_8(HOMO)*	S_1^N
S^N_7(LUMO)*	1		
S^E_8(HOMO)*	0.00	1	
S_1^N	0.02	0.35	1

The associated statistical parameters of Eq. 1 indicate that this equation is statistically significant and that the variation of the numerical values of a group of three local atomic reactivity indices of atoms of the common skeleton explains about 95% of the variation of log(IC_{50}). Figure 3, spanning about 1.9 orders of magnitude, shows that there is a good correlation of observed *versus* calculated values and that almost all points are inside the 95% confidence interval. A very important point to stress is the following. When a local atomic reactivity index of an inner occupied MO (i.e., HOMO-1 and/or HOMO-2) or of a higher vacant MO (LUMO+1 and/or LUMO+2) appears in any equation, this means that the remaining of the upper occupied MOs (for example, if HOMO-2 appears, upper means HOMO-1 and HOMO) or the remaining of the empty MOs (for example, if LUMO+1 appears, lower means the LUMO) contribute to the interaction. Their absence in the equation only means that the variation of their numerical values does not account for the variation of the numerical value of the biological property.

Results for Case 2. The common skeleton for this case is shown below (Fig. 4).

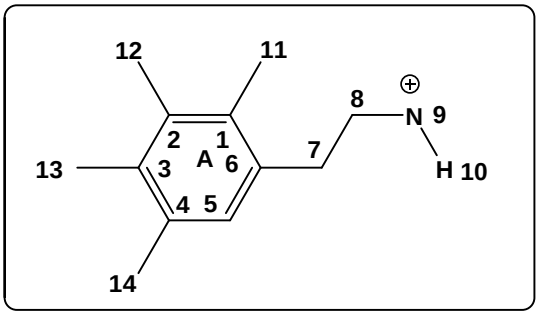

Figure 4: Common skeleton numbering for case 2

The best equation obtained was:

$$\log(IC_{50}) = -1.59 + 2.08 S^N_7(\text{LUMO})^* - 0.44 S^E_3 + 0.004 S^N_4 - 0.08 \eta_{13} \quad (2)$$

with n=24, R=0.96, R^2=0.93, adj-R^2=0.91, F(4,19)=58.742 (p<0.000001) and SD=0.20. No outliers were detected and no residuals fall outside the ±2σ limits. Here, S^N_7(LUMO)* is the nucleophilic superdelocalizability of the lowest vacant MO localized on atom 7, S^E_3 is the total atomic electrophilic superdelocalizability of atom 3 and η_{13} is the local atomic hardness of atom 13. Tables 4 and 5 show the beta coefficients, the results of the t-test for significance of coefficients and the matrix of squared correlation coefficients for the variables of Eq. 2. There are no significant internal correlations between independent variables (Table 5). Figure 5 displays the plot of observed *vs.* calculated log(IC_{50}).

Table 4: Beta coefficients and t-test for significance of coefficients in Eq. 2

Var.	**Beta**	**t(19)**	**p-level**
S^N_7(LUMO)*	0.77	12.06	<0.000001
S^E_3	-0.40	-6.29	<0.000005
S^N_4	0.30	3.81	<0.001
η_{13}	-0.23	-2.87	<0.01

Table 5: Matrix of squared correlation coefficients for the variables in Eq. 2

	S^N_7(LUMO)*	S^E_3	S^N_4	η_{13}
S^N_7(LUMO)*	1			
S^E_3	0.02	1		
S^N_4	0.00	0.01	1	
η_{13}	0.00	0.00	0.35	1

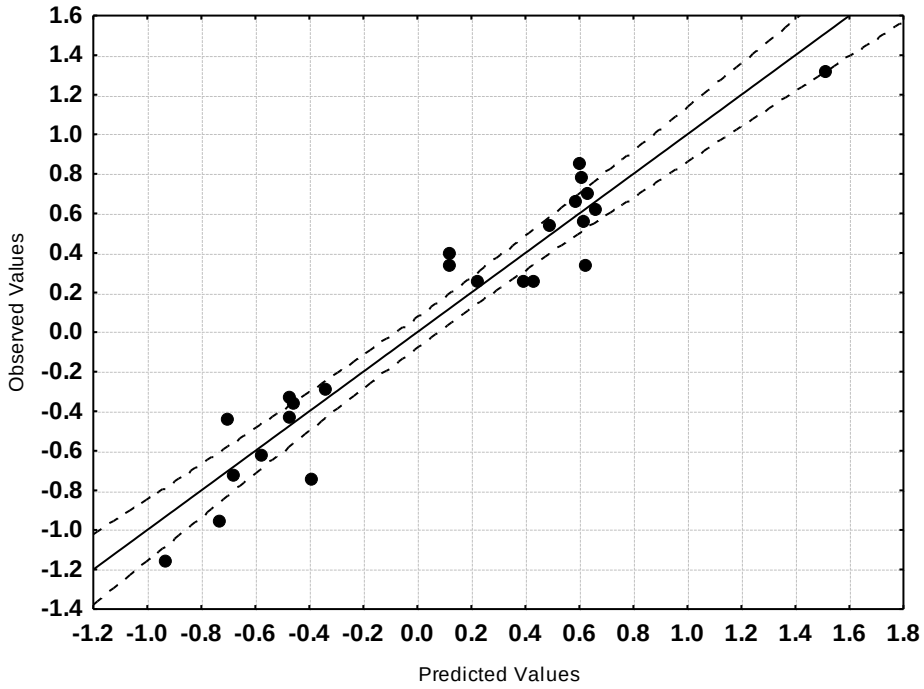

Figure 5: Plot of predicted vs. observed log(IC_{50}) values (Eq. 2). Dashed lines denote the 95% confidence interval

The associated statistical parameters of Eq. 2 indicate that this equation is statistically significant and that the variation of the numerical values of a group of four local atomic reactivity indices of atoms of the common skeleton explains about 91% of the variation of log(IC_{50}). Figure 5, spanning about 2.5 orders of magnitude, shows that there is a good correlation of observed *versus* calculated values and that almost all points are inside the 95% confidence interval.

Results for Case 3. The common skeleton is shown below (Fig. 6).

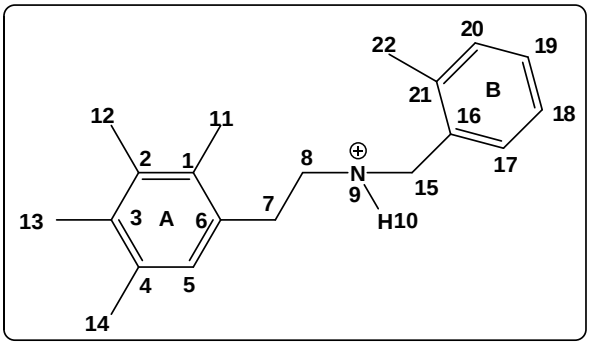

Figure 6: Common skeleton numbering for case 3

The best equation obtained was:

$$\log(IC_{50}) = -1.73 - 11.94 s_{11} + 0.18\eta_8 - 72.20 S^E_{15}(HOMO)^* \quad (3)$$

with n=12, R=0.98, R^2=0.96, adj-R^2=0.94, F(3,8)=59.151 (p<0.00001) and SD=0.08. No outliers were detected and no residuals fall outside the ±2σ limits. Here, s_{11} is the local atomic softness of atom 11, η_8 is the local atomic hardness of atom 8 and S^E_{15}(HOMO)* is the electrophilic superdelocalizability of the highest occupied MO localized on atom 15. Tables 6 and 7 show the beta coefficients, the results of the t-test for significance of coefficients and the matrix of squared correlation coefficients for the variables of Eq. 3. There are no significant internal correlations between independent variables (Table 7). Figure 7 displays the plot of observed *vs.* calculated log(IC_{50}).

Table 6: Beta coefficients and t-test for significance of coefficients in Eq. 3

Var.	Beta	t(8)	p-level
s_{11}	-0.93	-12.12	<0.000002
η_8	0.49	6.434	<0.0002
S^E_{15}(HOMO)*	-0.19	-2.55	<0.03

Table 7: Matrix of squared correlation coefficients for the variables in Eq. 3

	s_{11}	η_8	S^E_{15}(HOMO)*
s_{11}	1		
η_8	0.06	1	
S^E_{15}(HOMO)*	0.01	0.01	1

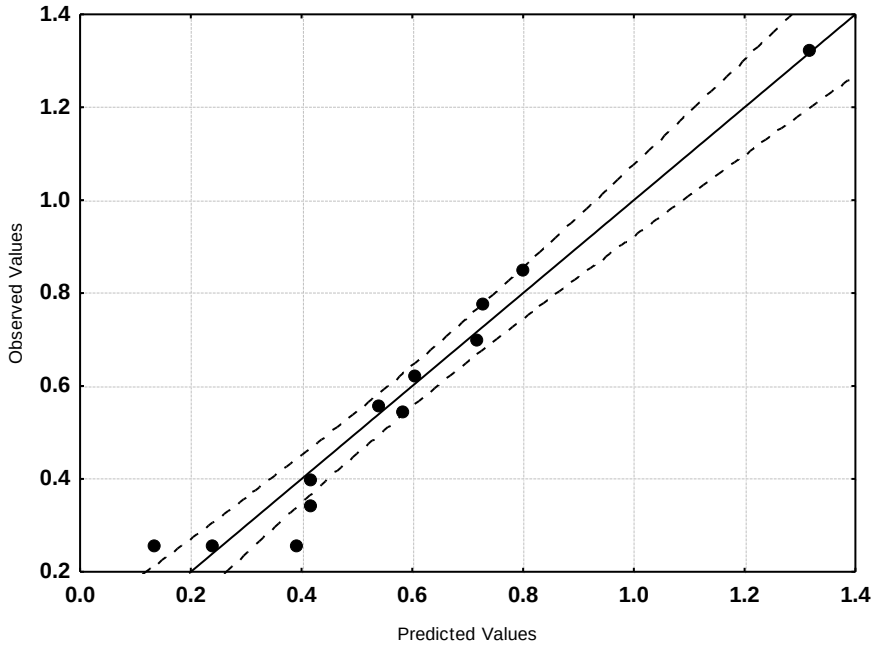

Figure 7: Plot of predicted vs. observed log(IC_{50}) values (Eq. 3). Dashed lines denote the 95% confidence interval

The associated statistical parameters of Eq. 3 indicate that this equation is statistically significant and that the variation of the numerical values of a group of three local atomic reactivity indices of atoms of the common skeleton explains about 94% of the variation of log(IC_{50}). Figure 7, spanning about 1.2 orders of magnitude, shows that there is a good correlation of observed *versus* calculated values and that almost all points are inside the 95% confidence interval.

Results for Case 4. The common skeleton for this case is shown below (Fig. 8).

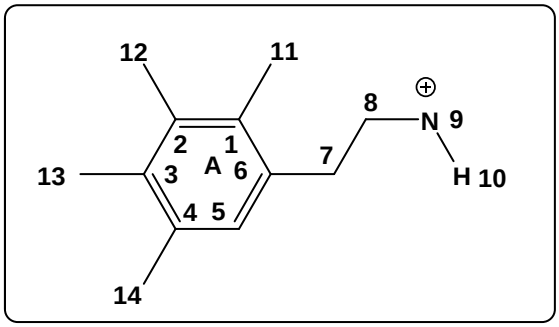

Figure 8: Common skeleton numbering for case 4

The best equation obtained was:

$$\log(IC_{50}) = 1.65 + 0.71 S_2^N(LUMO)^* - 0.10\eta_{13} \quad (4)$$

with n=12, R=0.88, R^2=0.85, adj-R^2=0.85, F(2,9)=33.247 (p<0.00007) and SD=0.19. No outliers were detected and no residuals fall outside the ±2σ limits. Here, S_2^N(LUMO)* is the nucleophilic superdelocalizability of the lowest vacant MO localized on atom 2 and η_{13} is the local atomic hardness of atom 13. Tables 8 and 9 show the beta coefficients, the results of the t-test for significance of coefficients and the matrix of squared correlation coefficients for the variables of Eq. 4. There are no significant internal correlations between independent variables (Table 9). Figure 9 displays the plot of observed *vs.* calculated log(IC_{50}).

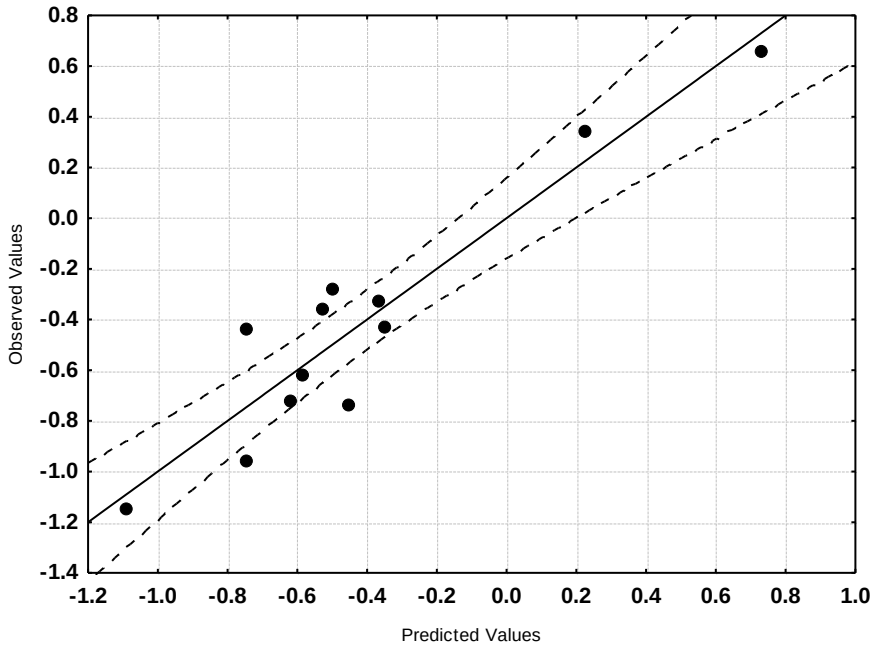

Figure 9: Plot of predicted vs. observed log(IC_{50}) values (Eq. 4). Dashed lines denote the 95% confidence interval

Table 8: Beta coefficients and t-test for significance of coefficients in Eq. 4.

Var.	Beta	t(9)	p-level
S_2^N(LUMO)*	0.81	6.93	<0.00007
η_{13}	-0.36	-3.12	<0.01

Table 9: Matrix of squared correlation coefficients for the variables in Eq. 4.

	S_2^N(LUMO)*	η_{13}
S_2^N(LUMO)*	1	
η_{13}	0.03	1

The associated statistical parameters of Eq. 4 indicate that this equation is statistically significant and that the variation of the numerical values of a group of two local atomic reactivity indices of atoms of the common skeleton explains about 85% of the variation of log(IC_{50}). Figure 9, spanning about 2.0 orders of magnitude, shows that there is a good correlation of observed *versus* calculated values and that almost all points are inside the 95% confidence interval. Table 10 shows the local molecular orbitals of some atoms appearing in Eqs. 1-4. Nomenclature: Molecule (molecule's HOMO) / (HOMO-2)* (HOMO-1)* (HOMO)* - (LUMO)* (LUMO+1)* (LUMO+2)*.

Table 10: Local molecular orbitals of atoms 2, 7, 8 and 15

Molecule	Atom 2	Atom 7	Atom 8	Atom 15
1π(66)	66π-68π	63σ-67σ	66σ-67σ	----
2π(57)	57π-59π	52σ-58σ	57σ-58σ	----
3 (53)	53π-55π	52σ-54σ	53σ-54σ	----
4 (57)	57π-59π	56σ-58σ	57σ-58σ	----
5 (98)	98π-101π	93σ-99σ	98σ-100σ	94σ-99σ
6 (89)	89π-92π	81σ-90σ	89σ-91σ	85σ-90σ
7 (85)	85π-88π	84σ-86σ	84σ-88σ	82σ-86σ
8 (89)	89π-92π	88σ-90σ	89σ-92σ	86σ-90σ
9 (49)	49π-51π	48σ-50σ	48σ-50σ	----
10π(75)	74π-77π	72σ-76σ	75σ-76σ	----
11π(60)	60π-61π	54σ-61σ	56σ-61σ	----
12π(61)	61π-63π	60σ-62σ	61σ-62σ	----
13 (81)	81π-84π	80σ-84σ	80σ-82σ	78σ-82σ
14 (107)	107π-110π	103σ-110σ	107σ-108σ	102σ-108
15 (92)	92π-93π	84σ-93σ	89σ-93σ	86σ-94σ
16 (93)	93π-96π	92σ-96σ	93σ-94σ	90σ-94σ
17 (65)	65π-67π	60σ-66σ	63σ-66σ	----
18 (69)	69π-71π	66σ-70σ	66σ-70σ	----
19 (69)	69π-71π	67σ-70σ	69σ-70σ	----
20π(57)	57π-59π	57σ-58σ	57σ-58σ	----
21π(97)	96π-100π	90σ-100σ	95σ-98σ	94σ-98σ
22π(97)	96π-100π	90σ-100σ	95σ-98σ	93σ-98σ
23 (101)	101π-104π	98σ-104σ	101σ-102σ	97σ-102σ
24 (89)	89π-92π	84σ-90σ	89σ-90σ	85σ-90σ

Discussion

Discussion of Case 1.

The Beta values (Table 2) show that the importance of variables in Eq. 1 is S^N_7(LUMO)*>> S^E_8(HOMO)*> S_1^N. The variable-by-variable (VbV) analysis of Eq. 1 shows that a high receptor affinity is associated with small values of S^N_7(LUMO)* if this index has positive values, with small negative values of and with large positive values for S_1^N. Atom 7 is a carbon atom of the side chain ring (Fig. 2). Table 10 shows that all MOs have a σ nature. Table 10 also shows that the local $HOMO_7$* is located quite far below from the molecule's HOMO. Therefore, this MO is not very reactive. If S^N_7(LUMO)* is positive, small values for this index are obtained by shifting upwards the energy of the

MO, making it less reactive (the same conceptual result is obtained if S^N_7(LUMO)* is negative). This result can be understood in two main ways. The first one is that this atom is engaged in a weak C-H….σ* dispersion interactions with the site using $HOMO_7$* [40]. The other one is that $(LUMO)_7$* could be engaged in a zero-electron repulsive interaction of the σ*-σ* kind [41, 42]. Let us remember that σ electrons are found in the methanediyl groups of some amino acids. On the other hand, and because atom 7 is bonded to the phenyl ring, there is a third possibility to consider. If the phenyl ring is engaged in a parallel π-π interaction with an aromatic moiety of the site but the rings are not exactly coincident among them, we may think in a C-H…π interaction [43]. What is really surprising is the role that this atom plays in regulating binding affinity. Note that all these interactions are weak. Atom 8 is the other carbon atom of the side chain, bonded to both, carbon atom 7 and nitrogen (Fig. 2). All its MOs have a σ nature (Table 10). In many cases but not all the local HOMO* and LUMO* coincide with the molecule's frontier MOs. S^E_8(HOMO)* is always negative. Therefore, to get smaller values for this index we must shift downwards the energy of the associated eigenvalue, making this MO less reactive. This suggests that $(HOMO)_8$* could be involved in a repulsive interaction with occupied MOs (of σ or π nature) of the site. Considering what we suggested about atom 7, it is more probable that this atom is also facing σ MOs. Atom 1 is a carbon atom of the aromatic ring (Fig. 2). This index is a scalar. High positive values for this index are obtained by lowering the empty MO energies, making this atom a good electron acceptor, probably from an occupied π MO of the receptor. Note that atom 1 is very close to atom 7. All the suggestions are displayed in the partial 2D pharmacophore of Fig. 10.

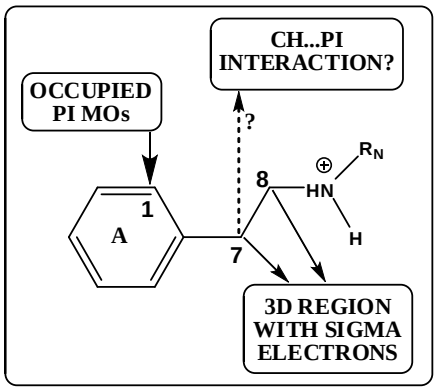

Figure 10: Partial 2D pharmacophore for Case 1

Discussion of Case 2

The Beta values (Table 4) show that the importance of variables in Eq. 2 is S^N_7(LUMO)*>> S^E_3> S^N_4> η_{13}. A high affinity is associated with low (positive) values of S^N_7(LUMO)*, low (negative) values of S^E_3, low (positive) values of S^N_4 and high (positive) values of η_{13}. Atom 7 is the carbon atom of the side chain bonded to the phenyl ring A (Fig. 4). The analysis of this index is exactly the same than for case 1. Atom 3 is a carbon atom in phenyl ring A (Fig. 4). Low negative vales are obtained by shifting downwards the energy of the HOMO (having the main numerical contribution to this index), making it less reactive. Therefore we suggest that this atom is interacting with an electron-rich center of the receptor. This interaction can be of the π-π or π-anion kinds but the fact that several atoms of ring A seem to interact with the receptor, a π-π interaction is more probable. Atom 4 is a carbon atom of the phenyl ring A (Fig. 4). Low values for S^N_4 are obtained by shifting upwards the empty MO energies, making these MOs less reactive. For this reason we suggest that atom 4 is interacting with an electron deficient center in the receptor. As in the case of atom 3, this interaction should be probably of the π-π kind (or π-cation). Atom 13 is the first atom of the R_3 substituent (Fig. 4). Table 1 shows that these substituents are of very different natures. High values of the *local* atomic hardness (η) of this atom are associated with high activity. η is defined as the HOMO*-LUMO* gap [6]. Large values for this index are obtained by lowering the (HOMO)* energy, rising the (LUMO)* energy or by both procedures. Technically this can be done by finding substitutions changing the localization of these MOs, without varying the electronic structure of ring A. The different nature of this atom (Table 1) makes it

difficult to suggest possible interactions. For example: the H atom may be involved in CH….X hydrogen bond, the halogen ones in halogen H-bonds, etc. We think that, if there are any interactions, they must be weak ones. This is so because a high value of η_{13} shows that atom 13 seems to resist exchanging electrons with the surroundings. This suggests that atom 13 is possibly positioned close to a hydrophobic moiety (an alkyl chain for example). All the suggestions are displayed in the partial 2D pharmacophore of Fig. 11.

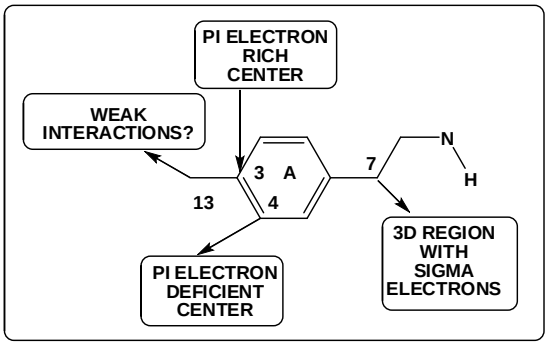

Figure 11: Partial 2D pharmacophore for Case 2

Discussion of Case 3

The Beta values (Table 6) show that the importance of variables in Eq. 3 is $s_{11} >> \eta_8 >> S^E_{15}(HOMO)^*$. A high affinity is associated with high (positive) values of s_{11}, low (positive) values of η_8 and small (negative) values of $S^E_{15}(HOMO)^*$. Atom 11 is the first atom of the R_1 substituent (Figs. 1 and 6, Table 1). s_{11} is defined as the inverse of η_{11} [6].Therefore a high positive value of s_{11} is equivalent to a small positive value of η_{11}. Then, a high binding affinity is related to a small (HOMO)*-(LUMO)* energy gap. Then, atom 11 is prone to exchange electrons with an electron-deficient center of the receptor site. This is in agreement with the fact that in all but two molecules this atom is an oxygen one. Atom 8 is a carbon atom of the side chain linking ring A with the N atom (Fig. 6). Low values of η_8 are associated with a high affinity. All local MOs have a σ nature. This suggests that atom 8 is prone to exchange electrons with the environment. Unhappily, η is a scalar that does not give much information about the nature of this electron exchange, but we may guess that it could be engaged in σ-σ*, σ*-σ and/or CH…X weak interactions. Atom 15 is a carbon atom linking the side chain with ring B (Fig. 6). Small (negative) values of $S^E_{15}(HOMO)^*$ are associated with a high receptor affinity. All local MOs have a σ nature. A low negative value for this index is obtained by lowering the value of the associated eigenvalue, making this MO less reactive. Therefore, we suggest that atom 15 is weakly interacting with the site through its lowest empty local MO. The interactions could be of the σ*-σ, σ*-π and/or C-H..X kinds. All the suggestions are displayed in the partial 2D pharmacophore of Fig. 12.

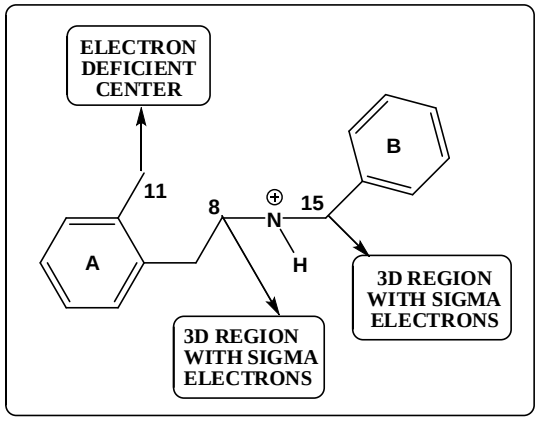

Figure 12: Partial 2D pharmacophore for Case 3

Discussion of Case 4

The Beta values (Table 8) show that the importance of variables in Eq. 4 is $S_2^N(LUMO)^* >> \eta_{13}$. A high affinity is associated with small values of $S_2^N(LUMO)^*$ is this index is positive and with large values of η_{13}. Atom 2 is a carbon atom in ring A (Fig. 8). Large positive values are obtained by shifting downwards the energy of the associated eigenvalue, making this MO more reactive. Therefore, we suggest that atom 2 is interacting with an electron-rich center. Atom 13 is the first atom of the R_3 substituent (Fig. 8). Large values of this index are associated with high binding affinity. The discussion of this index is the same than for Case 2 (see above). All the suggestions are displayed in the partial 2D pharmacophore of Fig. 13.

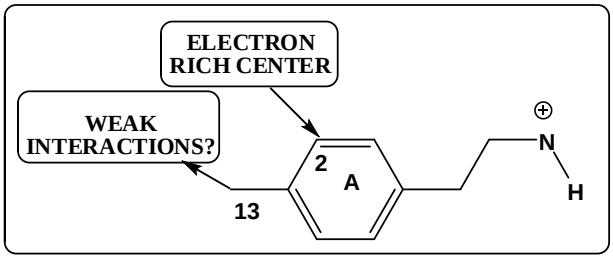

Figure 13: Partial 2D pharmacophore for Case 4

Integration of Results

Figure 14 shows the integration of the results of the four cases in a single interaction partial pharmacophore.

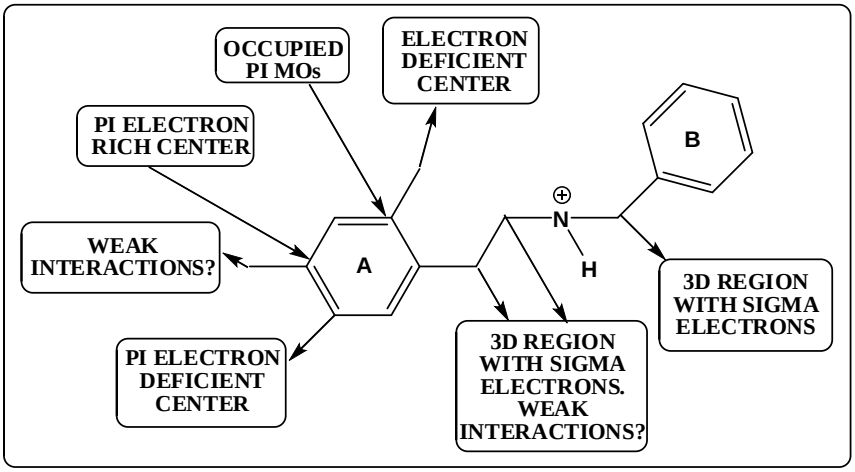

Figure 14: Integrated 2D partial interaction pharmacophore

Unhappily, our results did not include local atomic reactivity indices of ring B. But we noticed that the presence of ring B helps to change the localization of some occupied and empty MOs. N-2-methoxybenzyl-substituted analogs have a lesser affinity than their 2,5-dimethoxyphenethylamines counterparts. Therefore, it would be interesting to change ring B by smaller substituents carrying π electrons. The results about the apparent modulation of the receptor affinity by the sp^3 carbon atoms of the side chain is surprising. If this fact is real, then substituting these three carbon atoms with methyl groups and measuring by separate the activity of all optical isomers is another interesting possibility to test.

References.

1. Gómez-Jeria, J.S. On some problems in quantum pharmacology I. The partition functions. *International Journal of Quantum Chemistry* **1983,** 23, 1969-1972.
2. Peradejordi, F.; Martin, A.N.; Cammarata, A. Quantum chemical approach to structure-activity relationships of tetracycline antibiotics. *Journal of Pharmaceutical Sciences* **1971,** 60, 576-582.

3. Gómez-Jeria, J.S. Modeling the Drug-Receptor Interaction in Quantum Pharmacology. In *Molecules in Physics, Chemistry, and Biology*, Maruani, J., Ed. Springer Netherlands: 1989; Vol. 4, pp 215-231.
4. Gómez-Jeria, J.S.; Ojeda-Vergara, M. Parametrization of the orientational effects in the drug-receptor interaction. *Journal of the Chilean Chemical Society* **2003,** 48, 119-124.
5. Gómez-Jeria, J.S. *Elements of Molecular Electronic Pharmacology (in Spanish)*. 1st ed.; Ediciones Sokar: Santiago de Chile, 2013.
6. Gómez-Jeria, J.S. A New Set of Local Reactivity Indices within the Hartree-Fock-Roothaan and Density Functional Theory Frameworks. *Canadian Chemical Transactions* **2013,** 1, 25-55.
7. Gómez-Jeria, J.S.; Flores-Catalán, M. Quantum-chemical modeling of the relationships between molecular structure and in vitro multi-step, multimechanistic drug effects. HIV-1 replication inhibition and inhibition of cell proliferation as examples. *Canadian Chemical Transactions* **2013,** 1, 215-237.
8. Valdebenito-Gamboa, J.; Gómez-Jeria, J.S. A Theoretical Analysis of the Relationships between Electronic Structure and HIV-1 Integrase Inhibition, Antiviral Activity and Protein Binding Effects of a series of Naphthyridinone derivatives. *Der Pharma Chemica* **2015,** 7, 543-555.
9. Bravo, H.R.; Weiss-López, B.E.; Valdebenito-Gamboa, J.; Gómez-Jeria, J.S. A theoretical analysis of the relationship between the electronic structure of indole derivatives and their phytotoxicity against Lactuca Sativa seeds. *Research Journal of Pharmaceutical, Biological and Chemical Sciences* **2016,** 7, 792-798.
10. Gómez-Jeria, J.S.; Abarca-Martínez, S. A theoretical analysis of the cytotoxicity of a series of β-carboline-dithiocarbamate derivatives against prostatic cancer (DU-145), breast cancer (MCF-7), human lung adenocarcinoma (A549) and cervical cancer (HeLa) cell lines. *Der Pharma Chemica* **2016,** 8, 507-526.
11. Gómez-Jeria, J.S.; Bravo, H.R. A preliminary DFT analysis of phenolic acids in connection with their phytotoxic activity. *Der Pharma Chemica* **2016,** 8, 25-34.
12. Gómez-Jeria, J.S.; Castro-Latorre, P.; Kpotin, G. Quantum Chemical Analysis of the Relationships between Electronic Structure and Antiviral Activity against HIV-1 of some Pyrazine-1,3-thiazine Hybrid Analogues. *Der Pharma Chemica* **2016,** 8, 234-239.
13. Gómez-Jeria, J.S.; Cornejo-Martínez, R. A DFT study of the inhibition of human phosphodiesterases PDE3A and PDE3B by a group of 2-(4-(1H-tetrazol-5-yl)-1H-pyrazol-1-yl)-4-(4-phenyl)thiazole derivatives. *Der Pharma Chemica* **2016,** 8, 329-337.
14. Gómez-Jeria, J.S.; Gazzano, V. A quantum chemical study of the inhibition of α-glucosidase by a group of oxadiazole benzohydrazone derivatives. *Der Pharma Chemica* **2016,** 8, 21-27.
15. Gómez-Jeria, J.S.; Kpotin, G.A. A note on the inhibition of steroid 11β-hydroxylase, aldosterone synthase and aromatase by a series of coumarin derivatives *Der Pharma Chemica* **2016,** 8, 213-226.
16. Gómez-Jeria, J.S.; Latorre-Castro, P. On the relationship between electronic structure and carcinogenic activity in substituted Benz[a]anthracene derivatives. *Der Pharma Chemica* **2016,** 8, 84-92.
17. Gómez-Jeria, J.S.; Matus-Perez, M. A quantum chemical analysis of the inhibition of protein kinase A (PKA) and Rho-associated protein kinase-2 (ROCK2) by a series of urea-based molecules. *Der Pharma Chemica* **2016,** 8, 1-11.
18. Gómez-Jeria, J.S.; Moreno-Rojas, C. A theoretical study of the inhibition of human 4-hydroxyphenylpyruvate dioxygenase by a series of pyrazalone-quinazolone hybrids. *Der Pharma Chemica* **2016,** 8, 475-482.
19. Gómez-Jeria, J.S.; Orellana, Í. A theoretical analysis of the inhibition of the VEGFR-2 vascular endothelial growth factor and the anti-proliferative activity against the HepG2 hepatocellular carcinoma cell line by a series of 1-(4-((2-oxoindolin-3-ylidene)amino)phenyl)-3-arylureas. *Der Pharma Chemica* **2016,** 8, 476-487.
20. Gómez-Jeria, J.S.; Salazar, R. A DFT study of the inhibition of FMS-like tyrosine kinase 3 and the antiproliferative activity against MV4-11 cells by N-(5-(tert-butyl)isoxazol-3-yl)-N'-phenylurea analogs. *Der Pharma Chemica* **2016,** 8, 1-9.

21. Kpotin, G.; Atohoun, S.Y.G.; Kuevi, U.A.; Kpota-Hounguè, A.; Mensah, J.-B.; Gómez-Jeria, J.S. A Quantum-Chemical study of the Relationships between Electronic Structure and Trypanocidal Activity against Trypanosoma Brucei Brucei of a series of Thiosemicarbazone derivatives. *Der Pharmacia Lettre* **2016,** 8, 215-222.
22. Kpotin, G.A.; Atohoun, G.S.; Kuevi, U.A.; Houngue-Kpota, A.; Mensah, J.-B.; Gómez-Jeria, J.S. A quantum-chemical study of the relationships between electronic structure and anti-HIV-1 activity of a series of HEPT derivatives. *Journal of Chemical and Pharmaceutical Research* **2016,** 8, 1019-1026.
23. Gómez-Jeria, J.S.; Robles-Navarro, A. A Density Functional Theory and Docking study of the Relationships between Electronic Structure and 5-HT_{2B} Receptor Binding Affinity in N-Benzyl Phenethylamines. *Der Pharma Chemica* **2015,** 7, 243-269.
24. Gómez-Jeria, J.S.; Robles-Navarro, A. A Note on the Docking of some Hallucinogens to the 5-HT_{2A} Receptor. *Journal of Computational Methods in Molecular Design* **2015,** 5, 45-57.
25. Gómez-Jeria, J.S.; Robles-Navarro, A. DFT and Docking Studies of the Relationships between Electronic Structure and 5-HT_{2A} Receptor Binding Affinity in N-Benzylphenethylamines. *Research Journal of Pharmaceutical, Biological and Chemical Sciences* **2015,** 6, 1811-1841.
26. Gómez-Jeria, J.S.; Robles-Navarro, A. A Quantum Chemical Study of the Relationships between Electronic Structure and cloned rat 5-HT_{2C} Receptor Binding Affinity in N-Benzylphenethylamines. *Research Journal of Pharmaceutical, Biological and Chemical Sciences* **2015,** 6, 1358-1373.
27. Gómez-Jeria, J.S.; Morales-Lagos, D.R. Quantum chemical approach to the relationship between molecular structure and serotonin receptor binding affinity. *Journal of Pharmaceutical Sciences* **1984,** 73, 1725-1728.
28. Gómez-Jeria, J.S.; Morales-Lagos, D.; Rodriguez-Gatica, J.I.; Saavedra-Aguilar, J.C. Quantum-chemical study of the relation between electronic structure and pA2 in a series of 5-substituted tryptamines. *International Journal of Quantum Chemistry* **1985,** 28, 421-428.
29. Gómez-Jeria, J.S.; Morales-Lagos, D.; Cassels, B.K.; Saavedra-Aguilar, J.C. Electronic structure and serotonin receptor binding affinity of 7-substituted tryptamines. *Quantitative Structure-Activity Relationships* **1986,** 5, 153-157.
30. Gómez-Jeria, J.S.; Cassels, B.K.; Saavedra-Aguilar, J.C. A quantum-chemical and experimental study of the hallucinogen (±)-1-(2,5-dimethoxy-4-nitrophenyl)-2-aminopropane (DON). *European Journal of Medicinal Chemistry* **1987,** 22, 433-437.
31. Rickli, A.; Luethi, D.; Reinisch, J.; Buchy, D.; Hoener, M.C.; Liechti, M.E. Receptor interaction profiles of novel N-2-methoxybenzyl (NBOMe) derivatives of 2,5-dimethoxy-substituted phenethylamines (2C drugs). *Neuropharmacology* **2015,** 99, 546-553.
32. Note. The results presented here are obtained from what is now a routinary procedure. For this reason, we built a general model for the paper's structure. This model contains *standard* phrases for the presentation of the methods, calculations and results because they do not need to be rewritten repeatedly.
33. Frisch, M.J.; Trucks, G.W.; Schlegel, H.B.; Scuseria, G.E.; Robb, M.A.; Cheeseman, J.R.; Montgomery, J., J.A., et al. *G03 Rev. E.01*, Gaussian: Pittsburgh, PA, USA, 2007.
34. Gómez-Jeria, J.S. *D-Cent-QSAR: A program to generate Local Atomic Reactivity Indices from Gaussian 03 log files. v. 1.0*, v. 1.0; Santiago, Chile, 2014.
35. Gómez-Jeria, J.S. An empirical way to correct some drawbacks of Mulliken Population Analysis (Erratum in: J. Chil. Chem. Soc., 55, 4, IX, 2010). *Journal of the Chilean Chemical Society* **2009,** 54, 482-485.
36. Gómez-Jeria, J.S. *STERIC: A program for calculating the Orientational Parameters of the substituents* 2.0; Santiago, Chile, 2015.
37. Gómez-Jeria, J.S. Tables of proposed values for the Orientational Parameter of the Substituent. II. *Research Journal of Pharmaceutical, Biological and Chemical Sciences* **2016,** 7, 2258-2260.
38. Gómez-Jeria, J.S. Tables of proposed values for the Orientational Parameter of the Substituent. I. Monoatomic, Diatomic, Triatomic, n-CnH2n+1, O-n-CnH2n+1, NRR', and Cycloalkanes (with a single

ring) substituents. *Research Journal of Pharmaceutical, Biological and Chemical Sciences* **2016,** 7, 288-294.

39. Statsoft. *Statistica v. 8.0*, 2300 East 14 th St. Tulsa, OK 74104, USA, 1984-2007.
40. Alonso, M.; Woller, T.; Martín-Martínez, F.J.; Contreras-García, J.; Geerlings, P.; De Proft, F. Understanding the Fundamental Role of π/π, σ/σ, and σ/π Dispersion Interactions in Shaping Carbon-Based Materials. *Chemistry – A European Journal* **2014,** 20, 4845-4845.
41. Joselevich, E. Electronic Structure and Chemical Reactivity of Carbon Nanotubes: A Chemist's View. *ChemPhysChem* **2004,** 5, 619-624.
42. Joselevich, E. Chemistry and Electronics of Carbon Nanotubes Go Together. *Angewandte Chemie International Edition* **2004,** 43, 2992-2994.
43. Novoa, J.J.; Mota, F. The C–H···π bonds: strength, identification, and hydrogen-bonded nature: a theoretical study. *Chemical Physics Letters* **2000,** 318, 345-354.